Center for Turbulence Research
Proceedings of the Summer Program 1994

The coupling between flame surface dynamics and species mass conservation in premixed turbulent combustion

By A. Trouvé[1], D. Veynante[2], K. N. C. Bray[3] AND T. Mantel[4]

Current flamelet models based on a description of the flame surface dynamics require the closure of two inter-related equations: a transport equation for the mean reaction progress variable, $\widetilde{c}$, and a transport equation for the flame surface density, Σ. The coupling between these two equations is investigated using direct numerical simulations (DNS) with emphasis on the correlation between the turbulent fluxes of $\widetilde{c}$, $\overline{\rho u'' c''}$, and Σ, $\langle u'' \rangle_S \Sigma$. Two different DNS databases are used in the present work: a database developed at CTR by A. Trouvé and a database developed by C. J. Rutland using a different code. Both databases correspond to statistically one-dimensional premixed flames in isotropic turbulent flow. The run parameters, however, are significantly different, and the two databases correspond to different combustion regimes. It is found that in all simulated flames, the correlation between $\overline{\rho u'' c''}$ and $\langle u'' \rangle_S \Sigma$ is always strong. The sign, however, of the turbulent flux of $\widetilde{c}$ or Σ with respect to the mean gradients, $\partial \widetilde{c}/\partial x$ or $\partial \Sigma/\partial x$, is case-dependent. The CTR database is found to exhibit gradient turbulent transport of $\widetilde{c}$ and Σ, whereas the Rutland DNS features counter-gradient diffusion. The two databases are analyzed and compared using various tools (a local analysis of the flow field near the flame, a classical analysis of the conservation equation for $\widetilde{u'' c''}$, and a thin flame theoretical analysis). A mechanism is then proposed to explain the discrepancies between the two databases and a preliminary simple criterion is derived to predict the occurrence of gradient/counter-gradient turbulent diffusion.

1. Flame surface density and species mass evolution equations

The objective of theoretical descriptions of turbulent reacting flows is to provide tractable expressions for unclosed terms appearing in the conservation equations for mass, momentum, and energy. In the following, we focus our attention on mass conservation. In the classical theory of turbulent premixed flames, under the assumption of simple chemistry, the mass fractions of the reactive species are all linearly related and may be expressed in terms of a single reduced mass fraction called the reaction progress variable, $c = 1 - (Y_R/Y_{R,u})$, where Y_R is the fuel mass

1 Institut Francais du Pétrole, France
2 Laboratoire E.M2.C., C.N.R.S. and Ecole Centrale Paris, France
3 Cambridge University, U.K.
4 Center for Turbulence Research

fraction and $Y_{R,u}$ its value in the unburnt gas. The ensemble-averaged species mass balance is then written as:

$$\frac{\partial(\bar{\rho}\widetilde{c})}{\partial t} + \nabla.(\bar{\rho}\widetilde{\mathbf{U}}\widetilde{c}) + \nabla.(\overline{\rho\mathbf{u}''c''}) = \nabla.(\overline{\rho D\nabla c}) + \overline{\dot{\omega}}_R/Y_{R,u}, \tag{1}$$

where the tilde superscript denotes a Favre (density-weighted) average $\widetilde{Q} \equiv \overline{\rho Q}/\bar{\rho}$, the double prime symbol denotes the instantaneous deviation from the Favre average, $Q'' = Q - \widetilde{Q}$, D is the fuel mass diffusivity, and $\dot{\omega}_R$ represents the mass of fuel consumed by chemical reaction, per unit time and per unit volume.

In the flamelet theory for turbulent premixed combustion, the reaction zone is assumed to be a thin surface separating fresh and burnt gases. The local reaction rate may be expressed in terms of the local flame surface-to-volume ratio, Σ', and the ensemble-averaged reaction rate may be expressed in terms of the mean flame surface-to-volume ratio, also called the flame surface density, $\Sigma = \overline{\Sigma'}$ (Bray 1980, Williams 1985, Peters 1986):

$$\overline{\dot{\omega}_R} = \rho_u Y_{R,u} \langle S_C \rangle_S \, \Sigma, \tag{2}$$

where ρ_u is the density in the unburnt gas and $\langle S_C \rangle_S$ is the mean fuel consumption speed. The mean consumption speed accounts for local variations of the reaction rate along the flame surface while the flame surface density, Σ, characterizes the flame wrinkling due to the turbulent motions. For flames with Lewis numbers close to unity, $\langle S_C \rangle_S$ remains close to the laminar burning velocity s_L and to first order the mean reaction rate is proportional to Σ (Haworth & Poinsot 1992; Rutland & Trouvé 1993; Trouvé & Poinsot 1994). The $\widetilde{c}$-equation is then re-written as:

$$\frac{\partial(\bar{\rho}\widetilde{c})}{\partial t} + \nabla.(\bar{\rho}\widetilde{\mathbf{U}}\widetilde{c}) + \nabla.(\overline{\rho\mathbf{u}''c''}) = \nabla.(\overline{\rho D\nabla c}) + \rho_u s_L \Sigma. \tag{3}$$

In (3), the contribution of molecular diffusion is usually neglected for high Reynolds number flows and closure is only required to describe the turbulent flux of $\widetilde{c}$, $\overline{\rho\mathbf{u}''c''}$ and the flame surface density, Σ. A variety of modeling choices may be made for those terms ranging from standard gradient transport approximations for $\overline{\rho\mathbf{u}''c''}$ or simple algebraic closures for Σ, to full transport equations for both $\overline{\rho\mathbf{u}''c''}$ and Σ.

For instance, in the Coherent Flame Model (Marble & Broadwell 1977; Darabiha *et al.* 1987; Maistret *et al.* 1989; Candel *et al.* 1990) the flame surface density is obtained via a modeled formulation of an exact evolution equation called the Σ-equation (Pope 1988; Candel & Poinsot 1990):

$$\frac{\partial\Sigma}{\partial t} + \nabla.\widetilde{\mathbf{U}}\Sigma + \nabla.\langle\mathbf{u}''\rangle_S\Sigma + \nabla.\langle w\mathbf{n}\rangle_S\Sigma = \langle\kappa\rangle_S \, \Sigma, \tag{4}$$

where w is the flame front propagation speed, $\mathbf{n}$ is the flame normal vector pointing towards the fresh gases, κ is the flame stretch, and $\langle\ \rangle_S$ denotes a flame surface mean defined as an area-weighted ensemble-average (Pope 1988), $\langle Q\rangle_S \equiv \overline{Q\Sigma'}/\overline{\Sigma'} = \overline{Q\Sigma'}/\Sigma$. The three convective terms on the left-hand side of (4) are transport terms that correspond respectively to convection by the mean flow, turbulent diffusion,

and flame propagation. The term on the right-hand side of the equation is the source/sink term for flame surface density and accounts for production of flame surface area due to hydrodynamic straining and dissipation due to combined effects of flame propagation and flame surface curvature (Trouvé & Poinsot 1994). Different closure assumptions are required in the Σ-equation, in particular to calculate: the turbulent diffusion velocity, $\langle \mathbf{u}'' \rangle_S$, the transport due to flame propagation, $\langle w\mathbf{n} \rangle_S$, and the turbulent flame stretch, $\langle \kappa \rangle_S$ (see Duclos *et al.* (1993) for a critical review of the different formulations of the modeled Σ-equation that can be found in the literature).

While the need to model Σ through a transport equation has become increasingly recognized in recent years, the modeling of the turbulent flux of $\widetilde{c}$, $\overline{\rho \mathbf{u}'' c''}$, remains in comparison somewhat controversial. Using a standard gradient diffusion approximation (GD), one may write:

$$\overline{\rho u_i'' c''} = -\mu_t \frac{\partial \widetilde{c}}{\partial x_i}, \tag{5}$$

where μ_t is the turbulent viscosity.

Premixed flames, however, are known to exhibit counter-gradient diffusion (CGD) of mass reactant (Libby & Bray 1981; Bray *et al.* 1981). CGD is related to the differential effect of mean pressure gradients on cold, heavy reactants and hot, light products. This effect may be shown very simply under the classical Bray-Moss-Libby assumption of fresh reactants ($c = 0$) and fully burnt products ($c = 1$) separated by a thin flame sheet, leading to a bimodal probability density function of c. The x-component of the turbulent flux may then be written as (Bray 1980):

$$\overline{\rho u'' c''} = \overline{\rho} \widetilde{u'' c''} = \overline{\rho} \widetilde{c} (1 - \widetilde{c}) \left(\overline{U}_b - \overline{U}_u \right), \tag{6}$$

where $\overline{U}_b$ and $\overline{U}_u$ are respectively the x-component of the conditional mean velocity within burnt and unburnt gases. Thermal expansion and the associated flow acceleration through the flame will tend to make $\overline{U}_b$ greater than $\overline{U}_u$, thereby promoting counter-gradient turbulent diffusion of $\widetilde{c}$ ($\overline{\rho u'' c''} / \partial \widetilde{c} / \partial x > 0$, contrary to the predictions from Eq. (5)). Note that counter-gradient diffusion has been observed in a number of experiments (Moss 1980; Shepherd *et al.* 1982; Cheng & Shepherd 1991; Armstrong & Bray 1992).

While CGD has been extensively studied in the past ten years, the implications of this non-gradient transport phenomenon on the distribution of flame surface densities and the overall mean reaction rate remains unknown. In fact, a variety of conflicting modeling assumptions are still used in the current literature ranging from assumptions that simply neglect CGD and use standard gradient transport approximations as displayed in (5) (Darabiha *et al.* 1987; Maistret *et al.* 1989; Candel *et al.* 1990; Cant *et al.* 1990) to formulations where such approximations are carefully avoided and where closure is achieved by writing a transport equation for $\overline{\rho \mathbf{u}'' c''}$ (for instance in the Bray-Moss-Libby model: Bray 1980; Bray *et al.* 1989; Bray 1990).

It is important to realize that the closure assumptions required in the Σ-equation cannot be made independently of those required in the equation for $\widetilde{c}$. This may be best understood by considering the interdependence of Σ and $\widetilde{c}$. As seen in Eq. (3), Σ is a source term for $\widetilde{c}$ and the mean reaction progress variable will depend strongly on the distribution of flame surface densities. In addition, following Pope (1988), Σ may be expressed in terms of statistical properties of the c-field. For instance, the flame surface density is expressed as the product of the expected value for the magnitude of the gradient of c, conditioned on the flame surface, times the probability of being on that surface:

$$\Sigma = \langle |\nabla c| \mid c = c_f \rangle \; p(c_f), \tag{7}$$

where the flame is viewed as a surface-contour, $c = c_f$, and where $p(c_f)$ is the probability of $c = c_f$.

This theoretical coupling between Σ and $\widetilde{c}$ must have implications for models. Some of those implications are already well-known. For instance, in current models of the Σ-equation, while the turbulent transport, $\langle \mathbf{u}'' \rangle_S$, is described exclusively in terms of statistics of the turbulent flow field, the realizability of the combustion model is ensured by using a modeled expression for the flame stretch, $\langle \kappa \rangle_S$, that is $\widetilde{c}$-dependent. For instance, the closure model for $\langle \kappa \rangle_S$ leads to a vanishing Σ when the reaction reaches completion and $\widetilde{c}$ approaches unity.

The objective of the present work is to study further the exact implications of the coupling between the equations for Σ and $\widetilde{c}$. More specifically, direct numerical simulation (DNS) is used to determine: (1) if and under what conditions gradient-diffusion (GD) or counter-gradient diffusion (CGD) is observed in the $\widetilde{c}$-equation; (2) if there is any correlation between the turbulent flux of $\widetilde{c}$ and the turbulent flux of Σ, and in particular whether CGD (GD) in the $\widetilde{c}$-equation occurs with CGD (GD) in the Σ-equation.

2. Two different DNS databases

In the present work, two different direct numerical simulation databases are used. The first one, referenced as the CTR database, was developed at CTR by A. Trouvé and was previously used to study the statistics of the turbulent flame stretch, $\langle \kappa \rangle_S$, across the turbulent flame brush (Trouvé & Poinsot 1994). The CTR database was developed using a fully compressible, 3D, Navier-Stokes solver with one step irreversible chemistry. The numerical configuration corresponds to a premixed flame propagating in decaying isotropic turbulence. The ratio between the turbulent rms velocity and the laminar flame speed, u'/s_L, is set to an initial value of 10 and decreases to about 3 after four turbulent eddy turnover times. The second database was recently developed by C. J. Rutland (see Rutland & Cant 1994) using a low Mach number, 3D code. The Rutland code assumes a constant viscosity, whereas the CTR code features temperature-dependent transport coefficients. The numerical configuration corresponds to a premixed flame propagating in approximately stationary, weak turbulence, $u'/s_L \approx 1$. In the Rutland configuration, like in the CTR one, the simulated turbulent flame is statistically 1D. Comparisons between

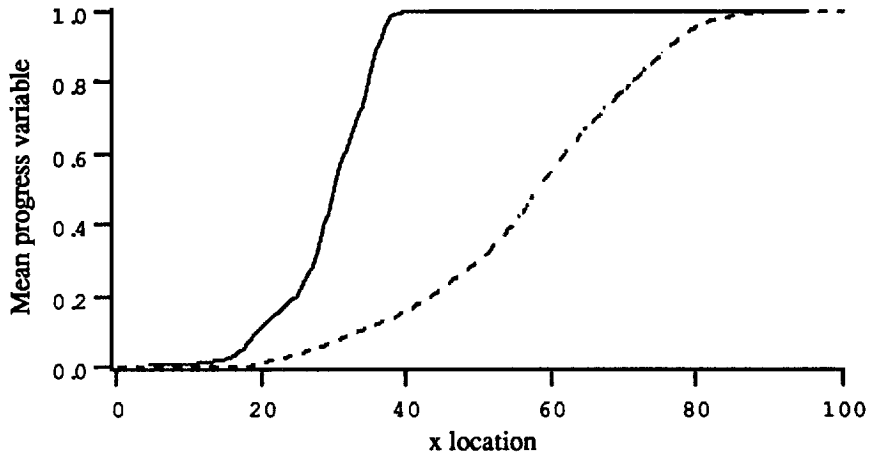

FIGURE 1. Comparison of the CTR and the Rutland DNS. The mean progress variable $\widetilde{c}$ is plotted as a function of x-location along the direction of mean propagation. The comparison is performed at a time selected so that the turbulent flame speed is approximately the same in both cases. Length scales are made nondimensional by the laminar flame thickness, δ_L. ——— : CTR database; ---- : Rutland database.

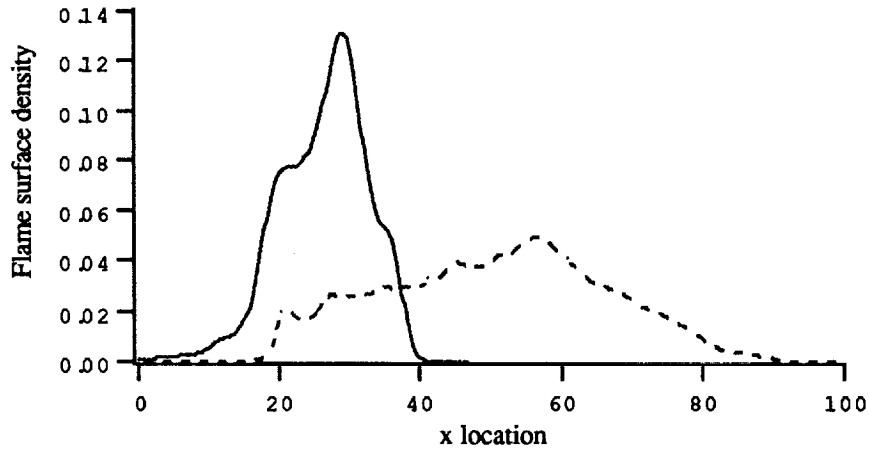

FIGURE 2. Comparison of the CTR and the Rutland DNS. The flame surface density Σ is plotted as a function of x-location along the direction of mean propagation. ——— : CTR database; ---- : Rutland database.

the two databases are performed assuming that the different computations correspond to the same laminar flame (same laminar flame thickness, δ_L, same laminar flame speed, s_L, and same molecular transport coefficients).

While the two databases feature turbulent flames with similar values of the turbulent flame speed, S_T, they also correspond to turbulent flames with significantly different structure. Fig. 1 shows two instantaneous profiles of the Favre-averaged progress variable $\widetilde{c}$ as a function of x-location along the direction of mean propagation. Fig. 2 presents a similar comparison for the flame surface density profiles. It is seen that the flame brush is about three times thicker in Rutland's database compared to the CTR case. Also, the flame front wrinkling, as measured by the magnitude of the flame surface density, is much greater in the CTR database. As seen in Fig. 3, the two DNS lie at different locations in the classical turbulent combustion diagram due to Borghi and Barrère (see Borghi 1985) and therefore correspond to different turbulent combustion regimes. The CTR database corresponds to flames that are more turbulent and feature smaller length scales. The box plotted in Fig. 3 corresponds to a zone where counter-gradient diffusion has been experimentally observed. Rutland's simulation lies in this zone, the CTR database lies outside. Note also that according to the Klimov-Williams criterion, the CTR database corresponds to non-flamelet combustion. Recent work by Poinsot *et al.* (1991) has shown that the domain of flamelet combustion is in fact significantly larger and the CTR database is within that domain according to the Poinsot *et al.* criterion (see Fig. 3).

The most interesting result is that the two databases display striking differences in their turbulent transport properties. Fig. 4 shows the turbulent flux $\overline{\rho u'' c''}$ as a function of the mean progress variable $\widetilde{c}$. Rutland's database exhibits counter-gradient turbulent diffusion of $\widetilde{c}$ ($\widetilde{\overline{\rho} u'' c''} > 0$), whereas gradient diffusion transport is found in the CTR database ($\widetilde{\overline{\rho} u'' c''} < 0$). These differences can be related to differences between the two codes (compressible/incompressible and variable/constant molecular transport coefficients), differences due to different initial and boundary conditions, or differences due to different values of the run parameters corresponding to different combustion regimes.

Figs. 5a and 5b present the spatial variations of different relevant mean flow velocities, $\widetilde{U}$, $\overline{U}_u$, $\overline{U}_b$, and $\langle u \rangle_S$, across the turbulent flame brush. In the Rutland simulation, the mean velocity within the products, $\overline{U}_b$, is always greater than the mean velocity within the reactants, $\overline{U}_u$, which according to (6) corresponds to counter-gradient turbulent diffusion of $\widetilde{c}$. In the CTR database, however, $\overline{U}_u$ is greater than $\overline{U}_b$, which again according to (6) corresponds to gradient turbulent diffusion. This last result may seem surprising since it is expected that the thermal expansion will induce a burnt gas velocity larger than the fresh gas velocity. It is worth emphasizing that conditional velocities may be difficult to interpret because the sampling is quite different for $\overline{U}_u$ and for $\overline{U}_b$. For example, at the leading edge of the turbulent flame brush, the flow field corresponds mainly to values of the progress variable $c = 0$, and the fresh gas conditional velocity, $\overline{U}_u$, is computed from a large number of samples. At that location, a few pockets have a value of

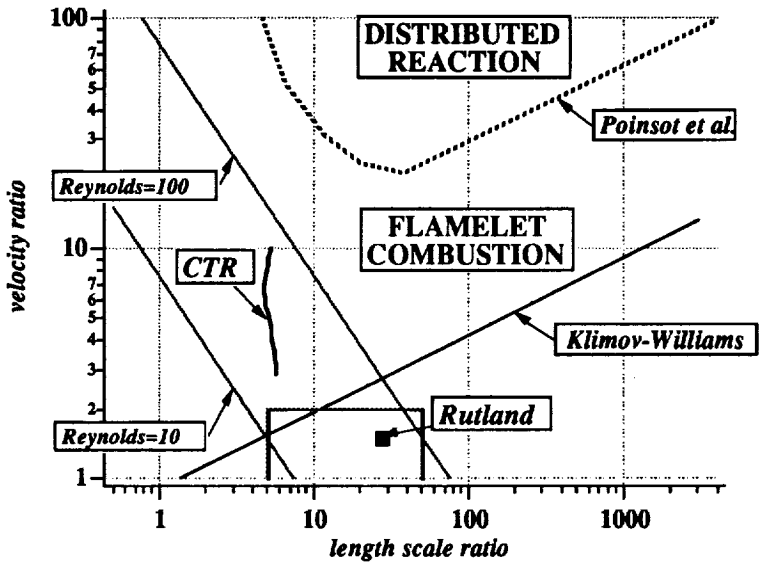

FIGURE 3. Premixed turbulent combustion diagram showing the different combustion regimes (from Borghi 1985; and Poinsot *et al.* 1991). The coordinates are the ratio of the turbulent length scale, l_t, and the laminar flame thickness, δ_l, and the ratio of the turbulent fluctuation, u', divided by the laminar flame speed, s_L. The parameters of the two DNS databases are plotted in the diagram.

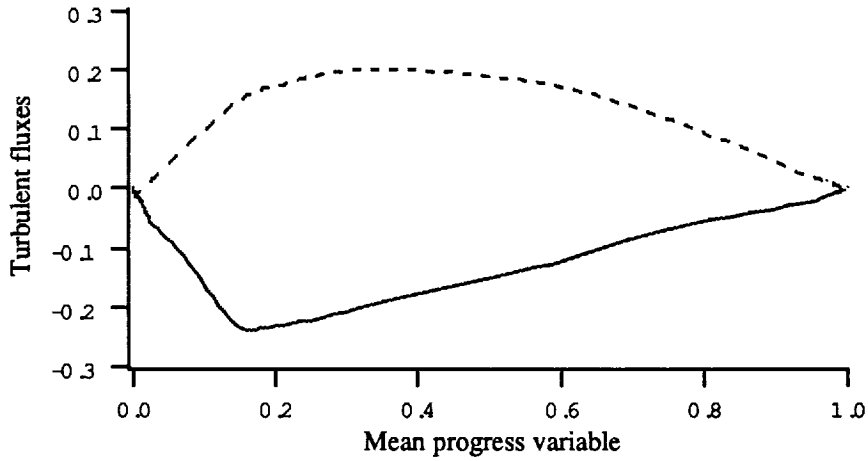

FIGURE 4. Comparison of the CTR and the Rutland DNS. The turbulent $\widetilde{c}$-flux, $\overline{\rho}\widetilde{u''c''}$, is plotted as a function of the mean reaction progress variable, $\widetilde{c}$. Velocities are made non-dimensional by the laminar burning velocity, s_L. ——— : CTR database; ---- ; Rutland database

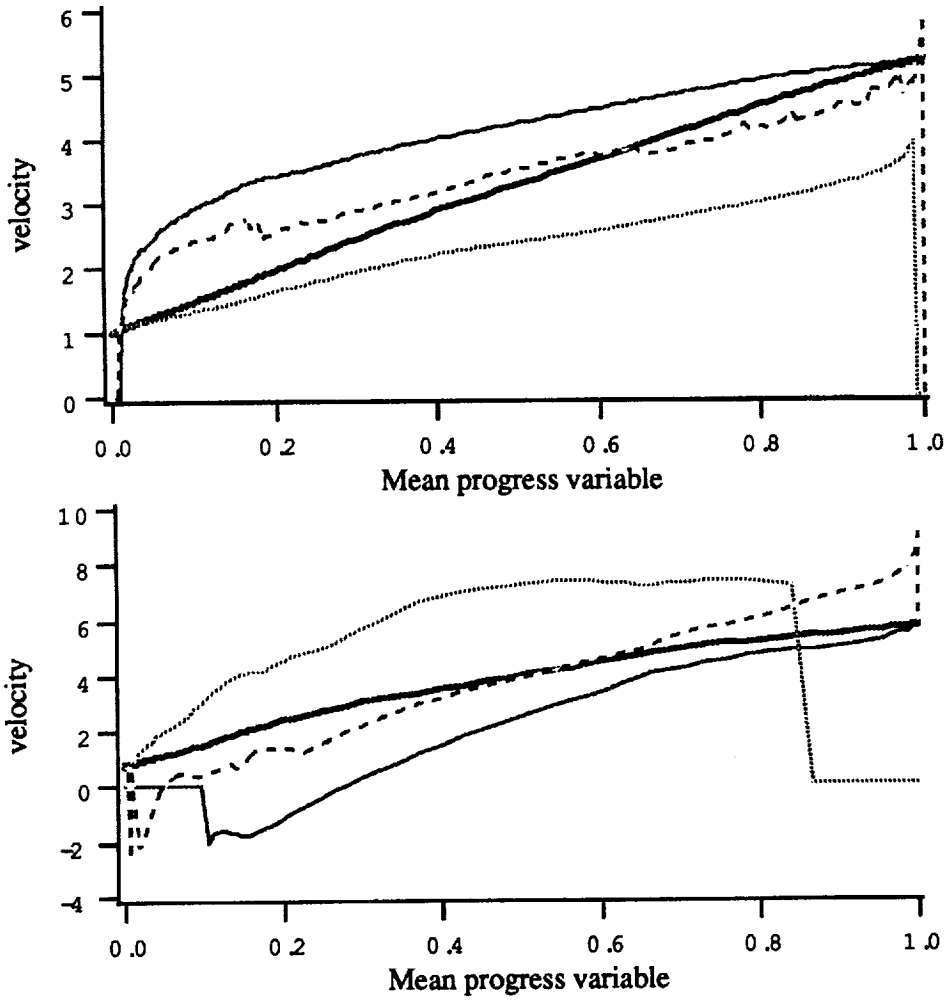

FIGURE 5. Mean flow velocities across the turbulent flame. The Favre-averaged velocity, $\widetilde{U}$, the conditional mean velocities, $\overline{U}_u$ and $\overline{U}_b$, and the surface-averaged velocity, $\langle u \rangle_S$, are plotted in $\widetilde{c}$-space. Velocities are made non-dimensional by the laminar burning velocity, s_L. Top: Rutland database. Bottom: CTR database. ——— : Favre average; ——— : products; ····· : reactants; ---- : $< u >_S$.

the progress variable $c = 1$, and $\overline{U}_b$ is determined from a small number of samples. The discrepancy between Figs. 5a and 5b is one of the keys to understanding when gradient or counter-gradient diffusion occurs and will be examined in further sections.

Different Lewis numbers Le (ratio of thermal to mass molecular diffusivities) have been investigated in the CTR database. Fig. 6 shows the spatial variations of the turbulent flux, $\widetilde{u''c''}$, across the turbulent flame brush at various times in the simulation, for two different Lewis numbers $Le = 0.8$ and $Le = 1.0$. In this figure, $\widetilde{u''c''}$ is made non-dimensional using the instantaneous rms turbulent velocity taken in the fresh gases. This non-dimensionalization allows separation of the decrease of the turbulent flux due to the decay of the turbulence from the variations due to other phenomena. Two different behaviors are observed. For $Le = 1.0$, the $\widetilde{u''c''}$-profile is changing rapidly during an initial phase and remains approximately constant after three eddy turnover times. In contrast, for $Le = 0.8$ the $\widetilde{u''c''}$-profile keeps changing in time and exhibits a continuous variation from negative towards positive values. These results are also shown in Fig. 7 where $\overline{\rho}\widetilde{u''c''}$ is first integrated across the turbulent flame brush and then plotted versus time. In Fig. 7, the $Le = 1$ flame reaches an asymptotic value, indicating thereby that no transition towards counter-gradient diffusion is to be expected and that a non-dimensional time of 4 is sufficient for data processing of the turbulent flame brush. Gradient turbulent transport observed in this case does not seem to be related to effects of initial conditions. For $Le = 0.8$, there is a clear trend towards transition to counter-gradient turbulent transport that might be related to thermal diffusive instabilities.

We now examine the idea that the differences in turbulent transport properties between the two databases are due to basic differences in the flame-flow dynamics (as opposed to numerical artifacts). These differences are further characterized using a local analysis of the flow field near the flame (section 3). Section 4 presents a comparison between the turbulent fluxes of $\widetilde{c}$ and Σ. A classical analysis of gradient versus counter-gradient turbulent diffusion based on the conservation equation for $\widetilde{u''c''}$ is presented in section 5. Finally, a theoretical analysis using a thin flame model is developed in section 6.

3. Local flow structure near the flame surface

As discussed in §2, the $Le = 1$ case from the CTR database and the Rutland simulation correspond to turbulent flames characterized by the same laminar flame thickness, δ_L, the same laminar burning velocity, s_L, the same molecular transport coefficients, but embedded in different turbulent flow fields. These simulated flames feature different global (spatially-averaged) properties, as illustrated in Figs. 1 and 2. A different perspective is adopted in this section where the flow velocity and the c-field are spatially resolved and analyzed in the vicinity of the reactive layers in a frame of reference attached to the flame. This frame of reference is used to determine, in particular, whether local flow variations occur in directions that are normal or tangential to the flame surface, *i.e.* whether local flow velocity gradients are aligned with local concentration gradients of reactive species.

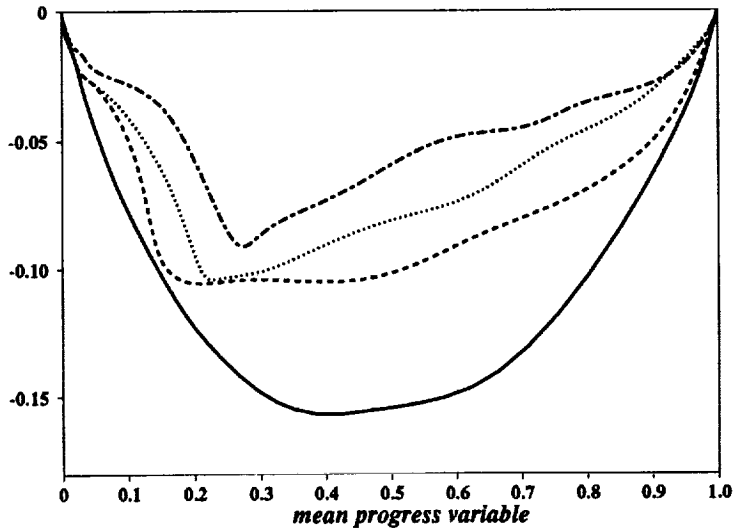

a)

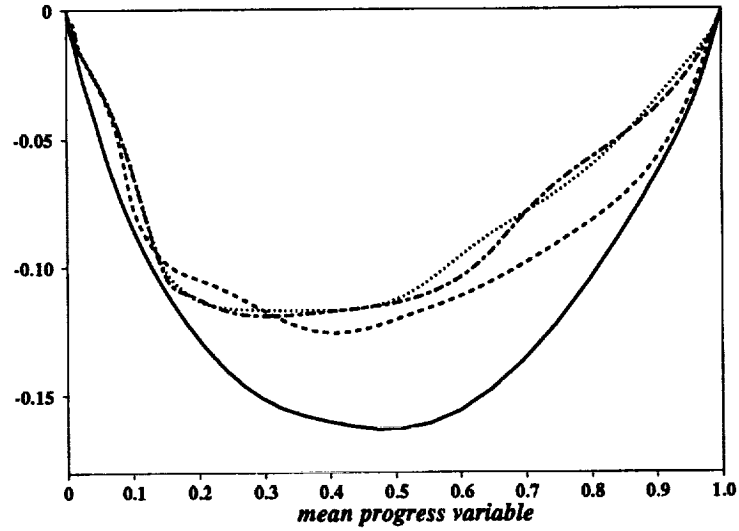

b)

FIGURE 6. Evolution of $\widetilde{u''c''}$ across the turbulent flame brush at different times in the simulations *a)* Le = 0.8; *b)* Le = 1.0. Time is made non-dimensional by the initial turbulent eddy turnover time. ——— : $t = 1.4$; ---- : $t = 2.7$; ····· : $t = 3.6$; —·— : $t = 4.5$.

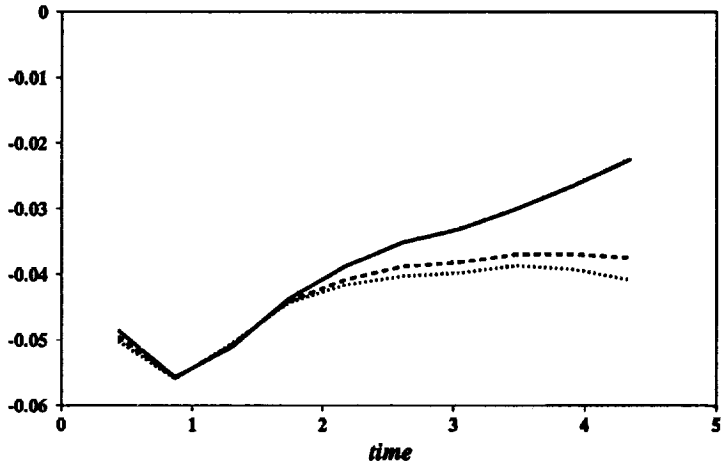

FIGURE 7. Evolution of the x-integral of $\overline{\rho u'' c''}$, integrated across the turbulent flame brush, versus time for different Lewis numbers ——— : $Le = 0.8$; ---- : $Le = 1.0$; ····· : $Le = 1.2$.

The flame-based analysis reveals that the local reaction rate profiles across the flame remain approximately uniform along the flame surface and are similar in the CTR and Rutland simulations. In other words, the local chemical structure of the flame remains laminar-like, a result that is consistent with a flamelet analysis and shows that the chemistry of such flames with unity Lewis number is relatively insensitive to flow perturbations. The local flow velocity profiles, however, exhibit striking differences, as discussed below.

Figs. 8a and 8b show the local flow dilatation across the flame at various locations along the flame surface, respectively for the Rutland and the CTR simulations. The dilatation of the flow is produced by both heat transfer in the flame preheat zone and heat release in the reaction zone. These local dilatation profiles remain approximately uniform along the flame surface and laminar-like in the Rutland simulation, whereas they exhibit more variations and significant deviations from the laminar case in the CTR simulation.

In the Rutland simulation, the flow field is found to be essentially one-dimensional and quasi-steady close to the flame. Most of the flame acceleration occurs along the flame normal direction:

$$\nabla.\mathbf{u} \approx \nabla(\mathbf{u}.\mathbf{n}).\mathbf{n}. \tag{8}$$

In that situation, the flow field within the flamelets is well described using the classical expressions that describe plane stretch-free laminar flames, where the flow velocity varies linearly with c in the flame normal direction:

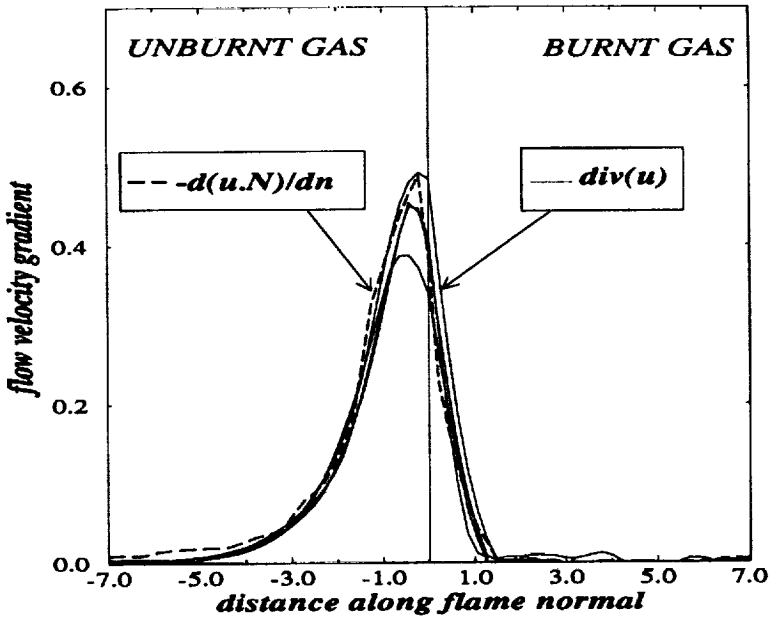

a)

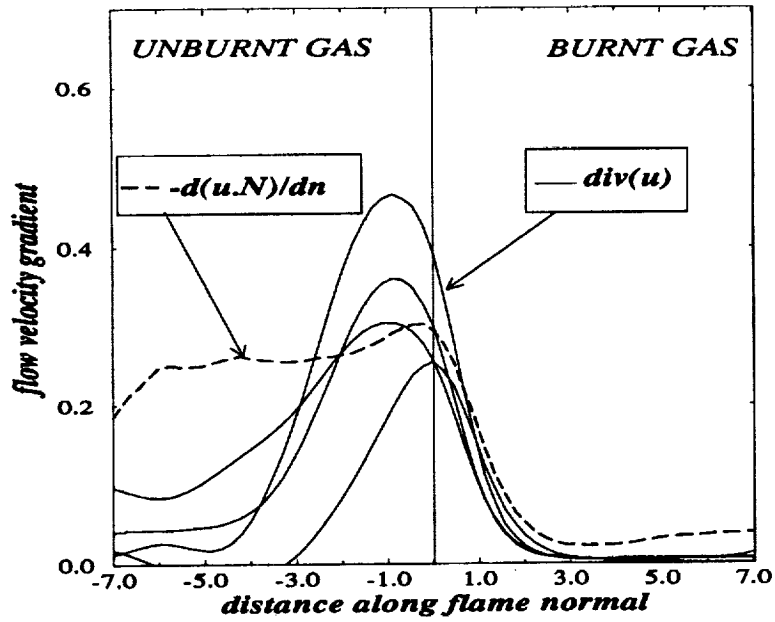

b)

FIGURE 8. A selection of local flow dilatation profiles normal to the turbulent flame for a) the Rutland database; b) the CTR database. In both figures, a local profile of the normal component of the flow velocity is also shown for comparison (a test of Eq. (8)). Quantities are made non-dimensional by the laminar burning velocity, s_L, and the laminar flame thickness, δ_L.

$$\mathbf{u}.\mathbf{n}(c) \approx \mathbf{u}.\mathbf{n}(c') + \tau(c' - c)s_L, \tag{9}$$

$$\mathbf{u}.\mathbf{t}(c) \approx \mathbf{u}.\mathbf{t}(c'), \tag{10}$$

where τ is the heat release factor, $\tau = T_b - T_u/T_u$, T_u, and T_b being respectively the temperature within fresh and burnt gases; $\mathbf{t}$ is a unit vector in the flame tangent plane. The relations (9) and (10) may be re-written as:

$$(\mathbf{u}.\mathbf{n}(c = 0.8) - \mathbf{u}.\mathbf{n}(c))/\tau s_L + 0.8 \approx c, \tag{11}$$

$$(\mathbf{u}.\mathbf{t}(c) - \mathbf{u}.\mathbf{t}(c = 0.8))/\tau s_L \approx 0. \tag{12}$$

Expressions (11) and (12) are found to provide good descriptions of the flow variations within the flamelets, as seen in Fig. 9a.

In the CTR simulation, however, the flow field is not one-dimensional and cannot be deduced directly from the dilatational field. Fig. 8b shows that (8) does not hold and Fig. 9b shows that the normal component of the flow velocity within the flamelets does not vary linearly with c; its gradient is not aligned with the gradient of c and exhibits large variations from one flame location to another. While in the Rutland simulation the flow field is determined by the dilatation occurring within the flame, the flow field in the CTR simulation appears dominated by the turbulent motions. These results will be used in section 6.

4. The relation between the turbulent fluxes of $\widetilde{c}$ and Σ

As shown in Fig. 4, the sign of the turbulent flux of $\widetilde{c}$ is different in the Rutland and CTR simulations. We now examine the turbulent flux of Σ, $\langle u'' \rangle_S \Sigma$. Fig. 10 shows that the CTR database features gradient diffusion transport for the flame surface density, whereas the Rutland database corresponds to counter-gradient diffusion. Note that since the turbulence intensities are higher in the CTR simulations, the magnitude of the turbulent fluxes are also found to be higher.

Following Bidaux and Bray (1994), an estimate of $\langle u \rangle_S$ is given by:

$$\langle u \rangle_S = \overline{U}_u + c^* \left(\overline{U}_b - \overline{U}_u \right), \tag{13}$$

where c^* is the progress variable level used to trace the flame front. This expression assumes a linear evolution of the mean velocity in the flame zone and is supported by Figs. 5a and 5b. Using the classical Bray-Moss-Libby (BML) relation $\widetilde{U} = (1 - \widetilde{c})\overline{U}_u + \widetilde{c}\overline{U}_b$, we can also write:

$$\langle u'' \rangle_S = \langle u \rangle_S - \widetilde{U} = (c^* - \widetilde{c}) \left(\overline{U}_b - \overline{U}_u \right). \tag{14}$$

Combining (6) and (14), we obtain:

$$\langle u'' \rangle_S \Sigma = \frac{(c^* - \widetilde{c})}{\widetilde{c}(1 - \widetilde{c})} \widetilde{u''c''} \Sigma, \tag{15}$$

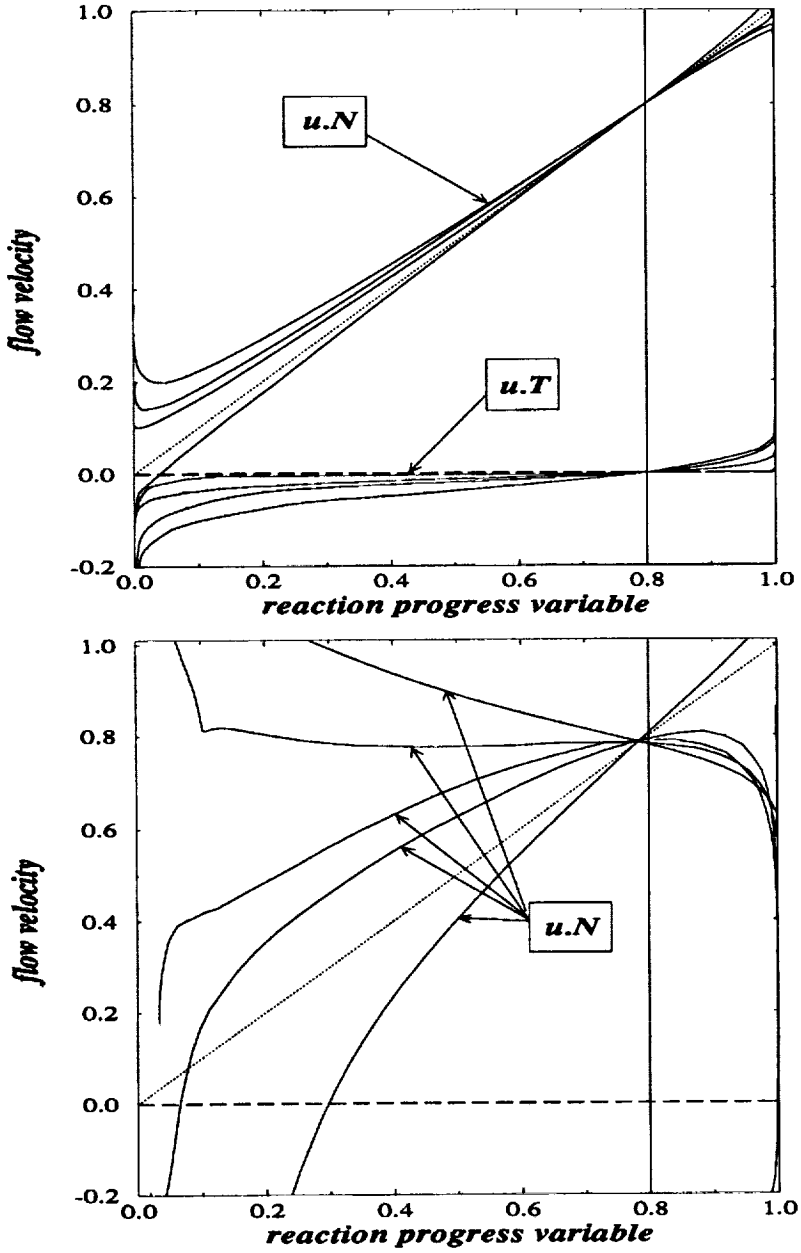

FIGURE 9. A selection of local profiles of the normal component of the flow velocity normal to the turbulent flame for a) the Rutland database; b) the CTR database (a test of Eq. (11)). The dotted line is the curve obtained for a plane, stretch-free laminar flame. In Fig. 9a, a selection of local profiles of the tangential component of the flow velocity is also shown for comparison (a test of Eq. (12)). Quantities are made non-dimensional by the laminar burning velocity, s_L, and the laminar flame thickness, δ_L.

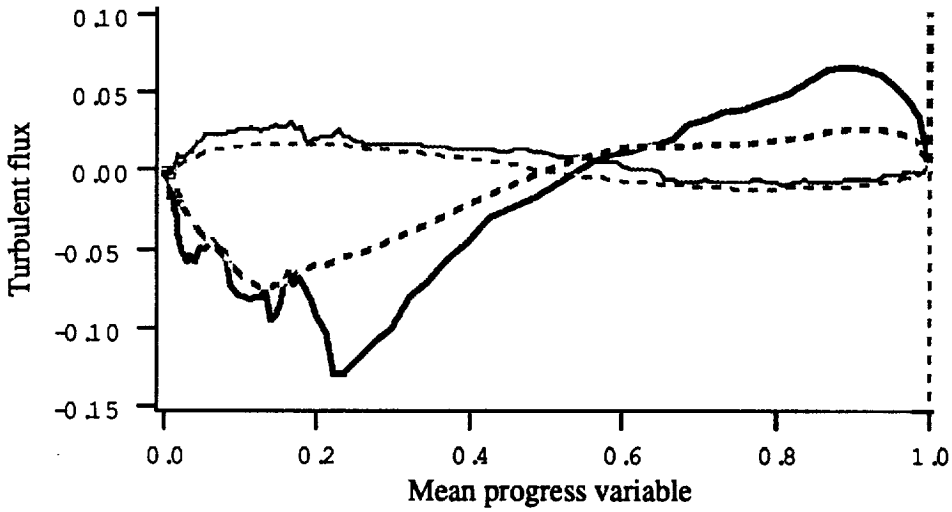

FIGURE 10. Comparison of the CTR and the Rutland DNS. The turbulent Σ-flux, $\langle u'' \rangle_S \Sigma$, is plotted as a function of the mean reaction progress variable, $\widetilde{c}$. Dashed lines corresponds to the estimate from Eq. (15) assuming $c^* = 0.5$. Velocities are made non-dimensional by the laminar burning velocity, s_L. ——— : CTR database; ——— : Rutland database.

which provides a simple relation between the turbulent fluxes for Σ and $\widetilde{c}$. This relation shows that $\langle u'' \rangle_S \Sigma$ and $\widetilde{u''c''}$ have the same sign at the leading edge of the turbulent flame, near $\widetilde{c} = 0$, and opposite signs on the burnt gas side, near $\widetilde{c} = 1$. Gradient (respectively counter-gradient) turbulent diffusion of the mean progress variable, $\widetilde{c}$, implies gradient (counter-gradient) turbulent diffusion of the flame surface density, Σ. The estimates obtained from Eq. (15) are also displayed in Fig. 10 and are seen to provide a very good estimate of $\langle u'' \rangle_S \Sigma$. In any case, the main result is that the turbulent diffusion term in the evolution equation for Σ is strongly correlated to the turbulent diffusion term in the equation for $\widetilde{c}$. In the following, we focus attention on the turbulent $\widetilde{c}$-flux.

5. Study of the transport equation for $\widetilde{u_i''c''}$

5.1 Preliminaries

To identify the physical phenomena responsible for turbulent diffusion of $\widetilde{c}$, a classical analysis consists of examining in detail the terms of the transport equation for the second order moment $\widetilde{u_i''c''}$. This balance equation can be obtained in a classical way from the continuity, the Navier-Stokes and the progress variable transport equations. After some algebra, the complete equation for $\widetilde{u_i''c''}$ may be expressed (Favre *et al.* 1976; Launder 1976):

$$\underbrace{\frac{\partial}{\partial t}\overline{\rho}\widetilde{u_i''c''}}_{\text{(I)}} + \underbrace{\frac{\partial}{\partial x_j}(\overline{\rho}\widetilde{U}_j\widetilde{u_i''c''})}_{\text{(II)}} = \underbrace{-\frac{\partial}{\partial x_j}\left(\overline{\rho}\widetilde{u_j''u_i''c''}\right)}_{\text{(III)}} \underbrace{-\overline{\rho}\widetilde{u_i''u_j''}\frac{\partial\widetilde{c}}{\partial x_j}}_{\text{(IV)}} \underbrace{-\overline{\rho}\widetilde{u_j''c''}\frac{\partial\widetilde{U}_i}{\partial x_j}}_{\text{(V)}}$$
$$\underbrace{-\overline{c''\frac{\partial\overline{p}}{\partial x_i}}}_{\text{(VI)}} \underbrace{-\overline{c''\frac{\partial p'}{\partial x_i}}}_{\text{(VII)}} \underbrace{-\overline{u_i''\frac{\partial\mathcal{J}_k}{\partial x_k}}}_{\text{(VIII)}} \underbrace{+\overline{c''\frac{\partial\tau_{ik}}{\partial x_k}}}_{\text{(IX)}} \underbrace{+\overline{\rho}\widetilde{u_i''\dot{\omega}}}_{\text{(X)}} \tag{16}$$

where $\mathcal{J}_k$ represents the molecular diffusion flux of c and τ_{ik} is the viscous stress tensor.

All the terms in (16) can be extracted from the simulations (including the unsteady term). For instance, Fig. 11 shows typical spatial variations of the different terms of (16), written for the x-component of the turbulent flux $\widetilde{u''c''}$, as obtained from the CTR database.

Fig. 11 shows that some of the terms in (16) are dominant and will determine the sign of $\widetilde{u''c''}$. The dominant contributions are due to the terms I, IV, VI, and VII. In the following section, our attention will be focused on the role played by these terms and their temporal evolution. Moreover, we have to notice that the imbalance term due to the inherent numerical approximations is one order of magnitude smaller than all the terms appearing in Eq. (16). This result is satisfactory and shows that the quality of the CTR database and that of the post-processing are sufficient to analyze the variations of second order moments.

5.2 Effect of the turbulence intensity and of the mean pressure gradient

In order to better understand the time evolution of $\widetilde{u''c''}$ (see Figs. 6 and 7), some terms in (16) are studied in more detail for two different Lewis numbers, $Le = 0.8$ and $Le = 1.0$. These terms are:

- the unsteady term I
- the production due to the interaction of the mean progress variable gradient and the turbulent flow field (term IV in (16)). Since this term is by definition always positive, it is responsible for gradient type diffusion.
- the production due to the mean pressure gradient (term VI in (16)) is supposed to be responsible for counter-gradient diffusion as pointed out by Libby & Bray (1981). These authors argue that the pressure gradient across the flame front preferentially accelerates the low density gases, creating a relative motion between fully burnt and fresh gases.
- the correlation between the fluctuations of the progress variable and the fluctuations of the pressure gradient (term VII). Little is known about this term which is usually considered as a dissipation term in non-reacting flows (Launder 1976).

Fig. 12 displays the time evolution of the terms I, IV, VI, and VII integrated across the turbulent flame brush ($\int_0^1 \frac{\partial}{\partial t}\overline{\rho}\widetilde{u_i''c''}d\widetilde{c}$, $\int_0^1 \overline{\rho}\widetilde{u''^2}\frac{\partial\widetilde{c}}{\partial x}d\widetilde{c}$, $\int_0^1 \overline{c''\frac{\partial\overline{p}}{\partial x}}d\widetilde{c}$ and $\int_0^1 \overline{c''\frac{\partial p'}{\partial x_i}}d\widetilde{c}$).

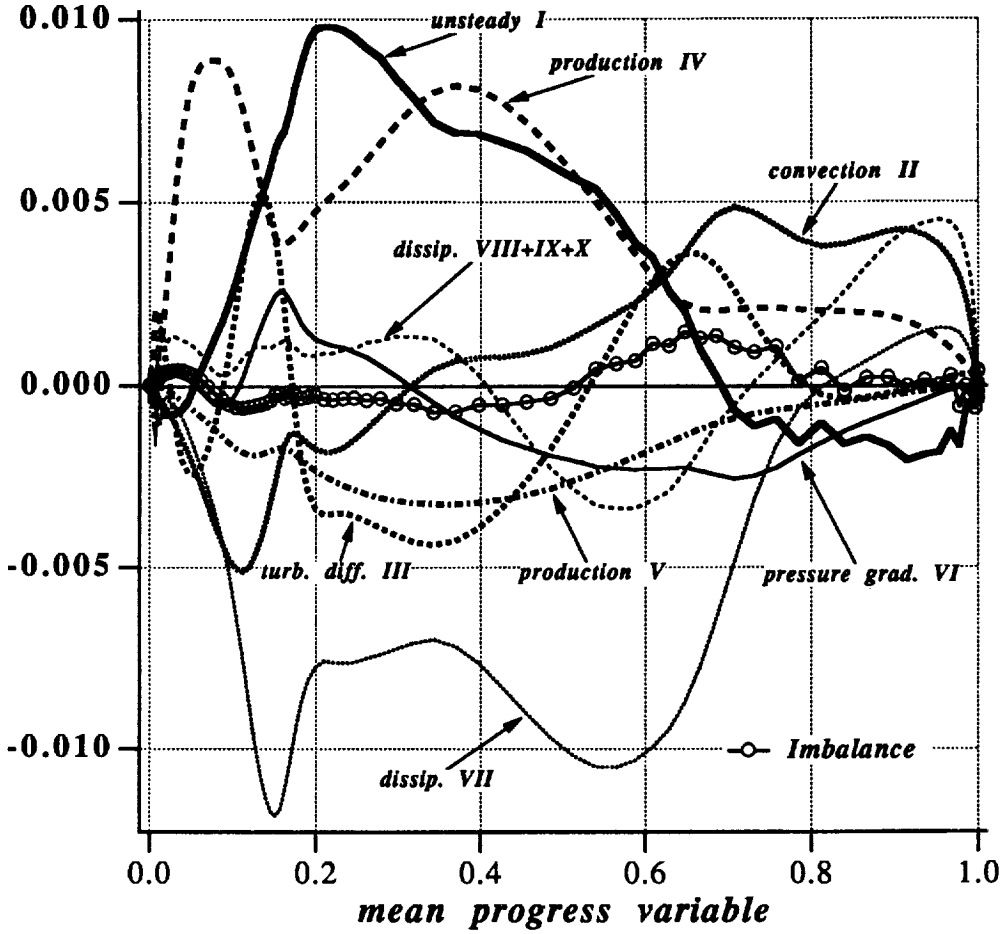

FIGURE 11. Spatial variations of the different terms in Eq. (16) versus $\widetilde{c}$, for the CTR case $Le = 1.0$ and $t/\tau_0 = 4.5$. The terms in (16) are made non-dimensional by $\rho_u \widetilde{u_u''^2}/l_{t_u}$. The curve with open circles correspond to the numerical errors that were found when closing the budget (16) and provides an estimate of the magnitude of the error for each term.

For both $Le = 0.8$ and $Le = 1.0$, the unsteady term I and the dissipation term VII behave in the same way. At early times, the unsteady term is negative producing counter-gradient diffusion and becomes positive later in the simulation playing the opposite role. The term VII is always negative in the simulations and acts to promote counter-gradient diffusion.

We now analyze the terms IV and VI which are supposed to be the key terms responsible for the turbulent gradient transport observed in the simulations. At initial times, both of these terms are positive and tend to produce gradient diffusion. Due to the high turbulence level (at $t/\tau_0 = 1.4$, $u'/s_L = 9.1$) and the relatively small thickness of the flame brush, the term IV appears to be the most dominant

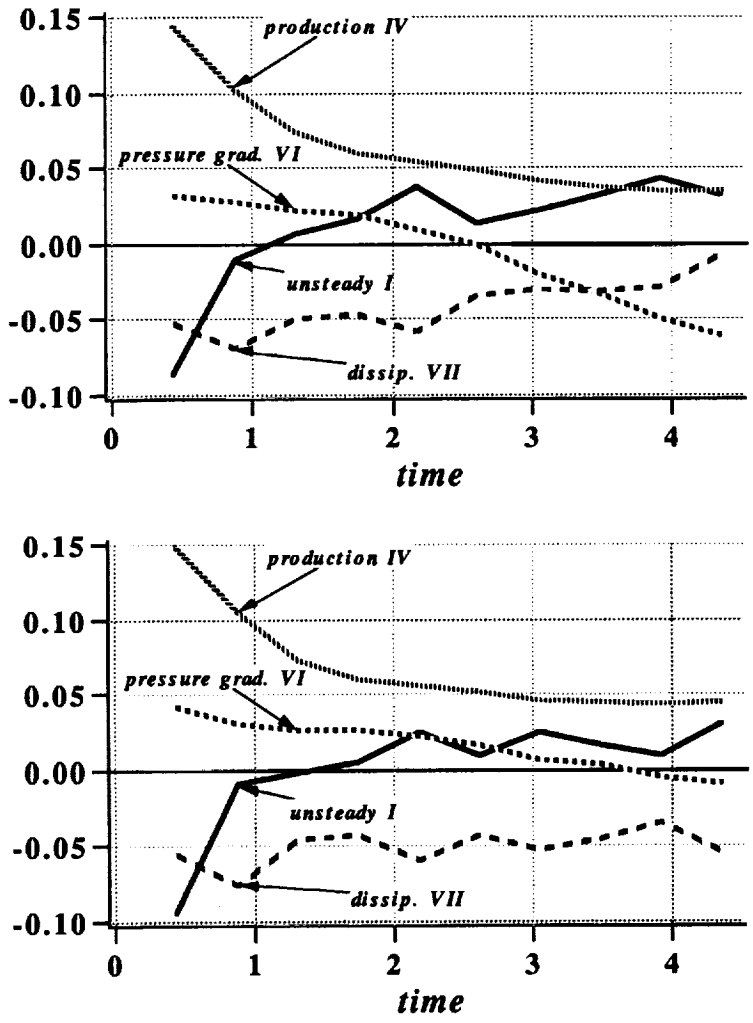

FIGURE 12. Time evolution of the terms I, IV, VI, and VII of Eq. (16) integrated across the turbulent flame brush, for (a) $Le = 0.8$ and (b) $Le = 1.0$. Terms I, IV, VI, and VII are made non-dimensional by the instantaneous value of $\rho_u \widetilde{u_u''^2}/l_{t_u}$. Time is made non-dimensional by the initial turbulent eddy turnover time.

term in (16). This result is consistent with the numerical study of Masuya (1986) who observes the flux becoming gradient diffusion type as the turbulence intensity increases.

As time proceeds, these two terms decrease continuously. While the term IV reaches an asymptotic value, the term VI changes sign and acts to promote counter-gradient diffusion. This feature is especially noticeable for the case $Le = 0.8$ where the term VI becomes the largest term in (16) after 4 turbulent eddy turnover time. This can be explained by the fact that for $Le = 0.8$ the turbulent flame speed is

much higher than in the case $Le = 1$ (Trouvé & Poinsot 1994) and consequently provokes a higher pressure jump across the turbulent flame which is approximately given by $\Delta p \sim \tau \rho_u S_T^2$.

5.3 Conclusions

At this point, we can tentatively conclude that the different behaviors for $\widetilde{u''c''}$ observed in the CTR database for $Le = 0.8$ and $Le = 1.0$ are essentially due to a higher mean pressure gradient in the case $Le = 0.8$, which is mainly due to a higher turbulent flame speed.

In a more general sense, it is well known experimentally that the turbulent flame speed, S_T, increases almost linearly with the turbulence intensity. Thus, the terms IV and VI are of the same order of magnitude and may even compensate themselves if the heat release parameter is sufficiently low (we can roughly estimate the ratio of the terms IV and VI to be of order τ^{-1}). This simplistic argument is in agreement with the work of Masuya (1986), who shows a stronger effect of τ compared to the effect of the ratio u'/s_L on the sign of $\widetilde{u''c''}$.

6. An analysis based on a thin flame model

6.1 An expression for turbulent diffusion transport

An analysis of the turbulent diffusion of the mean reaction progress variable may be conducted under the assumption of an infinitely thin flame front. Following Cant *et al.* (1990) or Trouvé and Poinsot (1994), the flame is viewed as a thin surface propagating towards the fresh gases with a velocity $\dot{\mathbf{X}}$ given by the sum of the fluid velocity and the flame propagation speed in the normal direction: $\dot{\mathbf{X}} = \mathbf{u} + w\mathbf{n}$. It may be shown that:

$$\frac{\partial \overline{c}}{\partial t} = \langle \dot{\mathbf{X}}.\mathbf{n} \rangle_S \Sigma = \langle \mathbf{u}.\mathbf{n} \rangle_S \Sigma + \langle w \rangle_S \Sigma, \tag{17}$$

where $\overline{c}$ is the Reynolds-averaged progress variable. This equation may be re-written as:

$$\frac{\partial \overline{c}}{\partial t} + \widetilde{\mathbf{U}}.\nabla \overline{c} = \langle \mathbf{u}.\mathbf{n} \rangle_S \Sigma + \langle w \rangle_S \Sigma + \widetilde{\mathbf{U}}.\nabla \overline{c}. \tag{18}$$

Using the geometrical relation $\nabla \overline{c} = -\langle \mathbf{n} \rangle_S \Sigma$, (17) becomes:

$$\frac{\partial \overline{c}}{\partial t} + \widetilde{\mathbf{U}}.\nabla \overline{c} = \langle \mathbf{u}''.\mathbf{n} \rangle_S \Sigma + \langle w \rangle_S \Sigma. \tag{19}$$

In the Bray-Moss-Libby theory, Reynolds and Favre averages of the progress variable c are related through the following expression: $\overline{c} = \overline{\rho c}/\rho_b$, where ρ_b is the mass density in the burnt gas. (18) and (19) can then be recast as transport equations for $\widetilde{c}$:

$$\frac{\partial \overline{\rho}\widetilde{c}}{\partial t} + \widetilde{\mathbf{U}}.\nabla \overline{\rho}\widetilde{c} = \rho_b \langle \mathbf{u}.\mathbf{n} \rangle_S \Sigma + \rho_b \langle w \rangle_S \Sigma + \widetilde{\mathbf{U}}.\nabla \overline{\rho}\widetilde{c}, \tag{20}$$

or

$$\frac{\partial \overline{\rho c}}{\partial t} + \widetilde{\mathbf{U}}.\nabla \overline{\rho c} = \rho_b \langle \mathbf{u}''.\mathbf{n} \rangle_S \Sigma + \rho_b \langle w \rangle_S \Sigma. \tag{21}$$

An exact equation for the Favre-averaged progress variable is:

$$\frac{\partial \overline{\rho}\widetilde{c}}{\partial t} + \nabla.\overline{\rho}\widetilde{\mathbf{U}}\widetilde{c} = -\nabla.\overline{\rho}\widetilde{\mathbf{u}''c''} + \langle \rho w \rangle_S \Sigma, \tag{22}$$

where molecular species diffusion and chemical reaction are included in $\langle \rho w \rangle_S$.

Combining (22) with (20) or (21), two expressions for the turbulent transport of $\widetilde{c}$ as a function of flame surface-averaged quantities are obtained:

$$-\nabla.\overline{\rho}\widetilde{\mathbf{u}''c''} = \rho_b \langle \mathbf{u}.\mathbf{n} \rangle_S \Sigma + (\rho_b \langle w \rangle_S - \langle \rho w \rangle_S) \Sigma + \nabla.\overline{\rho}\widetilde{\mathbf{U}}\widetilde{c}, \tag{23}$$

$$-\nabla.\overline{\rho}\widetilde{\mathbf{u}''c''} = \rho_b \langle \mathbf{u}''.\mathbf{n} \rangle_S \Sigma + (\rho_b \langle w \rangle_S - \langle \rho w \rangle_S) \Sigma + \overline{\rho c}\nabla.\widetilde{\mathbf{U}}. \tag{24}$$

These two expressions exhibit three contributions to the turbulent diffusion of $\widetilde{c}$. The first term on the right-hand side represents the correlation between the flame front movement and the velocity field. The second term involves the reaction rate, and the third term is clearly related to the thermal expansion. One may also note that with a model for the reaction rate, the only remaining unclosed term is $\langle \mathbf{u}''.\mathbf{n} \rangle_S$.

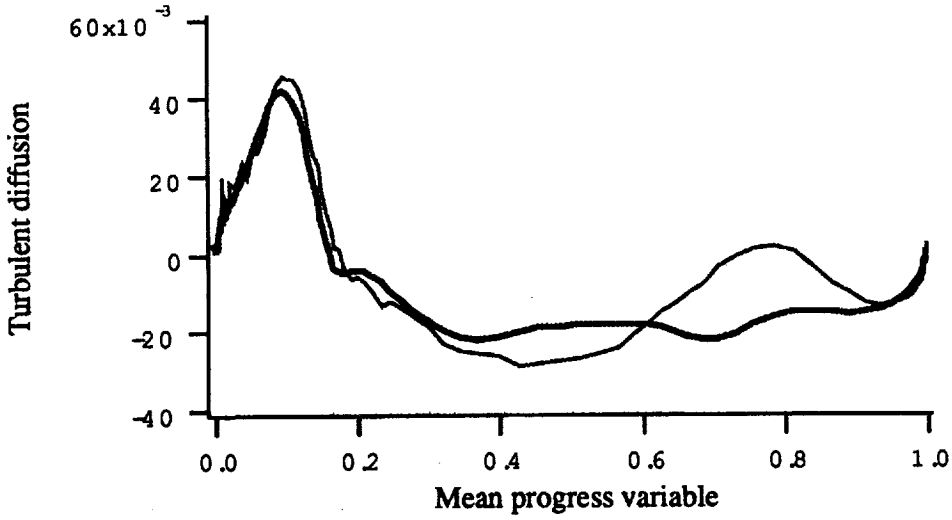

FIGURE 13. Comparison of the exact turbulent diffusion term $-\nabla.\overline{\rho}\widetilde{\mathbf{u}''c''}$ with its estimate from Eq. (23) in the CTR database. ——— : CTR database; ——— : estimation from (23).

Fig. 13 presents a comparison of the right-hand side and left-hand side of (23) in the CTR database ($Le = 1$). The agreement is quite good even though the probability density function of c is not fully bimodal in the database as assumed to derive expression (23). Fig. 14 shows the correlation $\langle \mathbf{u}.\mathbf{n} \rangle_S$ as a function of $\widetilde{c}$ for the two databases. This term is quite different in the two data sets. In the CTR database featuring a gradient turbulent transport, $\langle \mathbf{u}.\mathbf{n} \rangle_S$ decreases almost linearly with $\widetilde{c}$ from positive values near $\widetilde{c} = 0$ to negative ones near $\widetilde{c} = 1$. The positive values of $\langle \mathbf{u}.\mathbf{n} \rangle_S$ near $\widetilde{c} = 0$ correspond to local flow velocity vectors pointing into the reactants. At the leading edge, the flame front is convected towards fresh gases by the turbulent motions. This phenomenon accounts for the negative value of $\overline{U}_t$ seen in Fig. 5b. The product $\langle \mathbf{u}.\mathbf{n} \rangle_S \Sigma$ in (23) corresponds to a strong gradient trend (positive at the leading edge and negative at the trailing edge). On the other hand, in the Rutland database featuring a counter-gradient turbulent transport, $\langle \mathbf{u}.\mathbf{n} \rangle_S$ is negative with an almost constant value. In (23), the product $\langle \mathbf{u}.\mathbf{n} \rangle_S \Sigma$ is counter-gradient at the leading edge and becomes gradient at the trailing edge. Its effect is opposite to the one due to thermal expansion, $\nabla \overline{\rho} \widetilde{U} \widetilde{c}$.

Fig. 14 also shows the uncorrelated ($\langle \mathbf{u} \rangle_S . \langle \mathbf{n} \rangle_S$) and the correlated ($\langle \mathbf{u}.\mathbf{n} \rangle_S - \langle \mathbf{u} \rangle_S . \langle \mathbf{n} \rangle_S$) parts of the term $\langle \mathbf{u}.\mathbf{n} \rangle_S$. It is seen that $\mathbf{u}$ and $\mathbf{n}$ are mainly uncorrelated in the CTR database, whereas the correlation is not negligible in the Rutland case. This result is also in agreement with the local analysis developed in section 3.

6.2 Analysis of $\langle \mathbf{u}.\mathbf{n} \rangle_S$ and $\langle \mathbf{u}''.\mathbf{n} \rangle_S$ terms

From the previous analysis, the terms $\langle \mathbf{u}.\mathbf{n} \rangle_S$ and $\langle \mathbf{u}''.\mathbf{n} \rangle_S$ are found to be important ingredients of the turbulent transport of $\widetilde{c}$. Their trends are quite different in the two databases and provide a way to delineate between gradient and counter-gradient diffusion transport. As previously shown, the main differences between the two databases are the turbulence levels and the flame front wrinkling.

6.2.1 Low turbulence level

In the case of a low turbulence level and a low flame front wrinkling, $\langle \mathbf{u}.\mathbf{n} \rangle_S$ may be assumed almost constant and equal to its value at $\widetilde{c} = 0$ where the normal component is equal to -1 in the mean propagation direction x:

$$\langle \mathbf{u}.\mathbf{n} \rangle_S = -U_F, \tag{25}$$

where U_F is the flow velocity at the flame front and may be estimated with the same argument as previously used by Bidaux & Bray (1994) to derive an expression for the turbulent flux of flame surface density (Eq. (13)):

$$U_F = U_0 (1 + \tau c^*), \tag{26}$$

where U_0 is the fresh gases velocity and c^* the flame reference level. Assuming a stationary flame brush and using mass conservation, an estimate of $\langle \mathbf{u}.\mathbf{n} \rangle_S$ is:

$$\langle \mathbf{u}.\mathbf{n} \rangle_S = -\frac{\widetilde{U}}{(1 + \tau \widetilde{c})} (1 + \tau c^*), \tag{27}$$

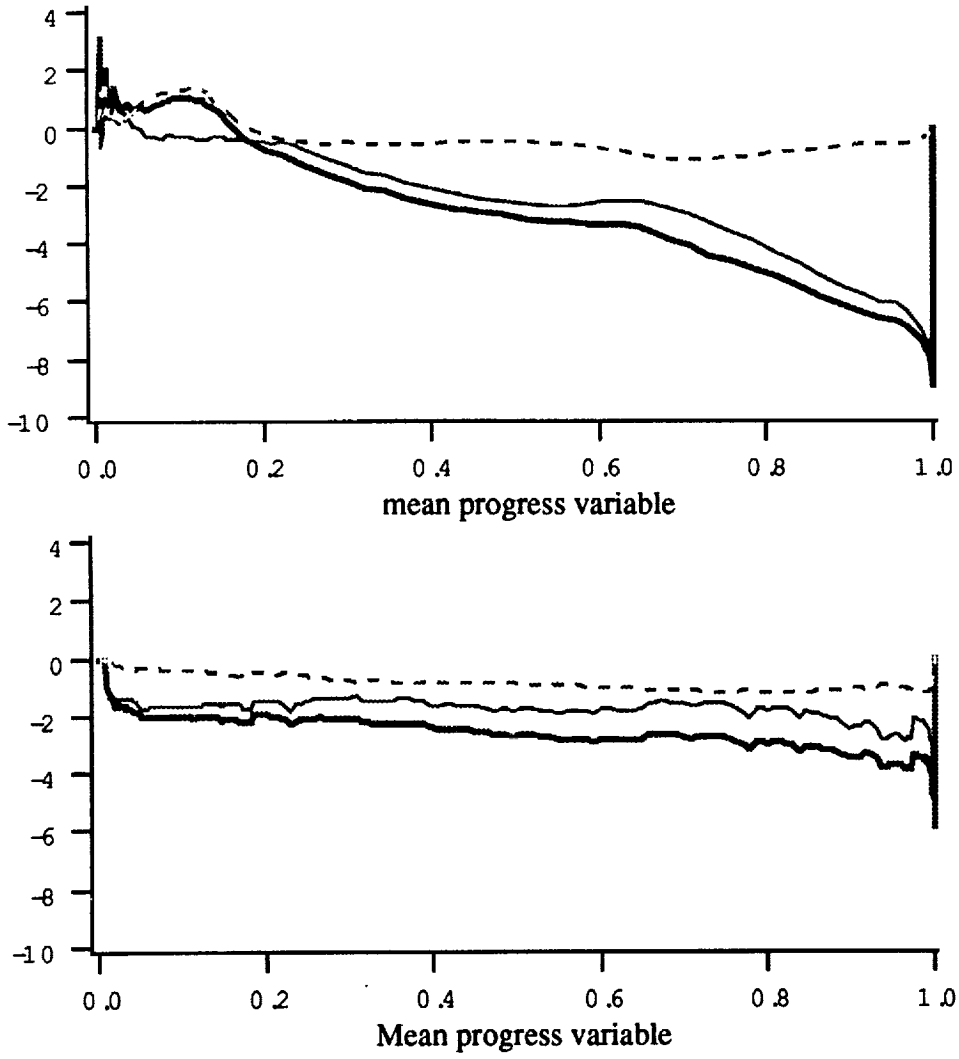

FIGURE 14. $\langle \mathbf{u}.\mathbf{n} \rangle_S$ (——), uncorrelated part $\langle \mathbf{u} \rangle_S . \langle \mathbf{n} \rangle_S$ (——), and correlated part $\langle \mathbf{u}.\mathbf{n} \rangle_S - \langle \mathbf{u} \rangle_S . \langle \mathbf{n} \rangle_S$ (----) plotted as a function of the mean progress variable, $\widetilde{c}$, for the two available databases (top: CTR, bottom: Rutland).

which is very well verified in the Rutland database. In this case, the flame front dynamics and the turbulent transport are mainly dominated by the mean flow

velocity and the thermal expansion.

6.2.2 High turbulence level

In the CTR database, the fluctuations at the flame front of the flow velocity and the flame normal vector may be assumed uncorrelated:

$$\langle \mathbf{u}''.\mathbf{n} \rangle_S \Sigma = \langle \mathbf{u}'' \rangle_S . \langle \mathbf{n} \rangle_S \Sigma. \tag{28}$$

Combining (28) and (15), it may be easily shown that:

$$\rho_b \langle \mathbf{u}''.\mathbf{n} \rangle_S \Sigma = -\frac{(c^* - \widetilde{c})}{\widetilde{c}(1-\widetilde{c})} \widetilde{u''c''} \frac{\partial \overline{\rho}\widetilde{c}}{\partial x}. \tag{29}$$

which suggests that $\langle \mathbf{u}''.\mathbf{n} \rangle_S$ might provide a way to analyze the turbulent diffusion transport of $\widetilde{c}$.

The only unclosed term in Eq. (24) is $\langle \mathbf{u}'' \rangle_S$. In the CTR DNS, the flame front movements are mainly dominated by the turbulent motions in the fresh gases (due to the higher viscosity, turbulent motions have a lower strength in the burnt gases). At the leading edge of the flame brush, the flame front is convected towards the fresh gases with a turbulent speed of the order of $-u'$ where u' is the turbulent rms velocity in the fresh gases. At the trailing edge, the flame front is convected towards the burnt gases by the most energetic turbulent eddies inside the fresh gases with a turbulent speed of the order of u'. Then, a simple model for $\langle \mathbf{u}'' \rangle_S$ is:

$$\langle \mathbf{u}'' \rangle_S = u'(2\widetilde{c} - 1), \tag{30}$$

which is in agreement with the CTR database as shown in Fig. 15.
From (28) and (30), one obtains:

$$\rho_b \langle \mathbf{u}''.\mathbf{n} \rangle_S \Sigma = -u'(2\widetilde{c} - 1) \nabla \overline{\rho}\widetilde{c}. \tag{31}$$

Using (29), assuming that $c^* = 0.5$, the turbulent flux of $\widetilde{c}$ becomes:

$$\widetilde{u''c''} = -2u'\widetilde{c}(1-\widetilde{c}), \tag{32}$$

which clearly corresponds to gradient turbulent transport.

6.2.3 Mechanisms for turbulent transport diffusion

From the previous analysis, the turbulent diffusion of $\widetilde{c}$ comes from two different mechanisms. The first one is the dynamics of the flame front itself, mainly due to thermal expansion. This phenomenon (clearly apparent in the term $\overline{\rho}\widetilde{c}\nabla.\widetilde{\mathbf{U}}$ of Eq. (24)) induces counter-gradient diffusions (CGD) as shown by the classical Bray-Moss-Libby expression (6). Due to thermal expansion and without any other effect, $\overline{U}_b$ is greater than $\overline{U}_u$ leading to CGD of $\widetilde{c}$.

In contrast, with a sufficiently high turbulence level, the flame front movement is dominated by the turbulent motions in the fresh gases as already seen in the CTR database. At the leading edge, the flame front is convected towards fresh gases, inducing negative velocities near the front, positive values of $\langle \mathbf{u}.\mathbf{n} \rangle_S$, and $\overline{U}_b$ lower

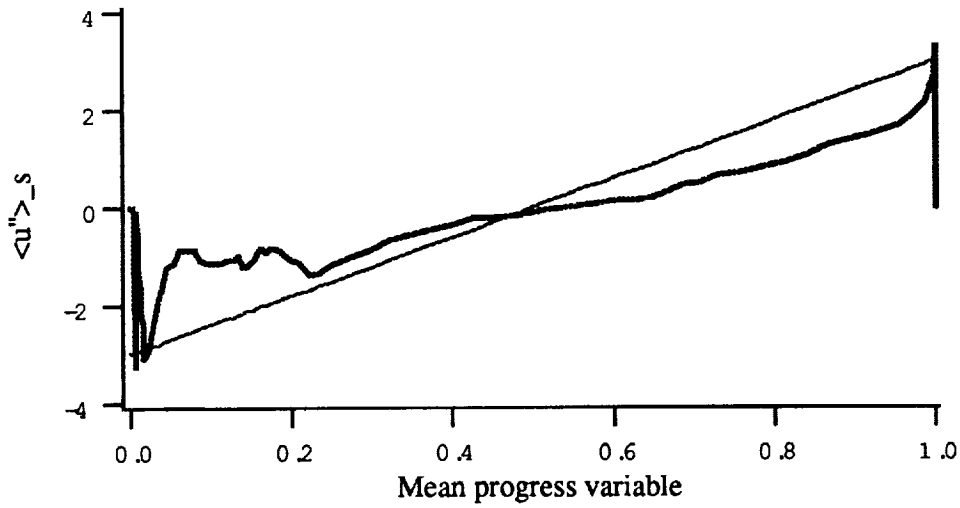

FIGURE 15. Comparison of $\langle \mathbf{u}'' \rangle_S$ and the modeled expression (30) in the CTR database. ——— : CTR database; ——— : estimation from (30).

than $\overline{U}_u$. At the trailing edge, intense turbulent motions in the fresh gases convect the flame front towards burnt gases and $\overline{U}_u$ is greater than $\overline{U}_b$ (see Fig. 16). In that case, the turbulent diffusion of $\widetilde{c}$ becomes gradient.

To summarize, with a high turbulence level, the flame front dynamics is dominated by the turbulent motions and the mean progress variable is similar to any passive scalar, leading to a classical gradient diffusion turbulent transport. With a low turbulence level, the intrinsic dynamics of the flame is important, and the mean progress variable cannot be reduced to a passive scalar. A counter-gradient diffusion turbulent transport is then encountered. It is well known that counter-gradient diffusion is promoted by a high heat release (i.e. a high value of τ). On the other hand, high turbulence levels induce gradient turbulent transport. The next step is to quantify the limits between gradient (GD) and counter-gradient (CGD) turbulent diffusion.

6.3 A criterion for gradient/counter-gradient turbulent diffusion

The objective is to derive a criterion for turbulent diffusion transport of the Favre-averaged mean progress variable, $\widetilde{c}$. Our analysis is based on Eq. (24). For GD, $-\nabla.\overline{\rho}\widetilde{\mathbf{u}''c''}$ has to be positive at the leading edge of the flame and negative at the trailing edge. As previously shown, this term may be expressed as the sum of three contributions. At the trailing edge, the first term, $\rho_b\langle \mathbf{u}''.\mathbf{n}\rangle_S\Sigma$, is negative, the second one, $(\rho_b\langle w\rangle_S - \langle \rho w\rangle_S J)\,\Sigma$ vanishes and has a higher order, and the third one, $\overline{\rho}\widetilde{c}\nabla.\widetilde{\mathbf{U}}$ is positive. Then, a necessary condition for GD is:

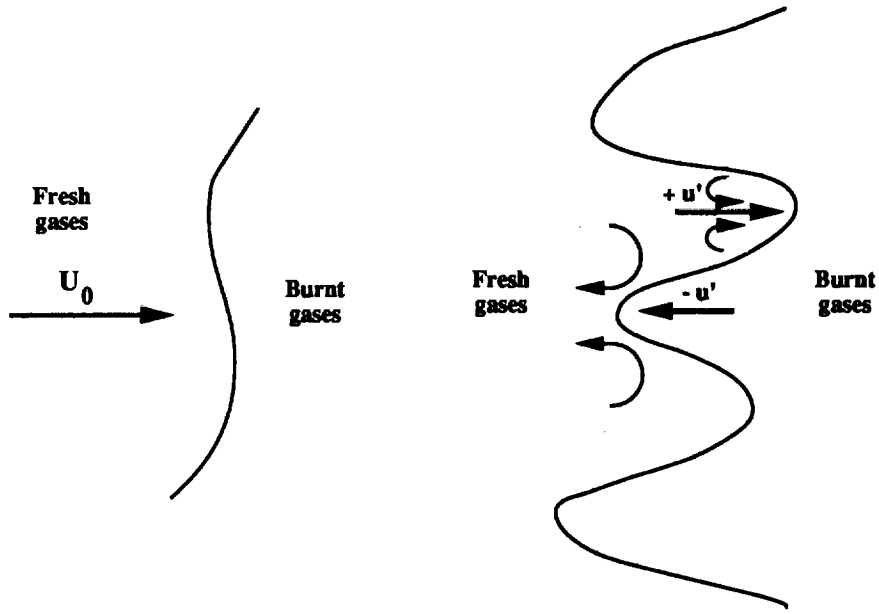

FIGURE 16. Mechanisms of counter-gradient (left) and gradient (right) turbulent diffusion transport for $\widetilde{c}$ and Σ.

$$\rho_b \left|\langle \mathbf{u}''.\mathbf{n}\rangle_S\right| \Sigma > \widehat{\overline{\rho} c} \nabla \widetilde{U}. \tag{33}$$

Some assumptions are now introduced to evaluate the terms appearing in (33). The mean velocity may be estimated by:

$$\widetilde{U} = U_0 + \tau S_T \widetilde{c}. \tag{34}$$

$\overline{\rho}$ is estimated from the Bray-Moss-Libby (BML) formulation:

$$\overline{\rho} = \frac{\rho_b (1+\tau)}{1+\tau\widetilde{c}}. \tag{35}$$

The BML algebraic closure for the flame surface density, Σ, is also used:

$$\Sigma = \frac{g}{\sigma_y L_y} \overline{c}(1-\overline{c}) = \frac{g}{\sigma_y L_y} \frac{1+\tau}{(1+\tau\widetilde{c})^2} \widetilde{c}(1-\widetilde{c}), \tag{36}$$

where L_y is the wrinkling scale of the flame front, g a model constant, and σ_y an orientation factor assumed to be a constant. The gradient of the mean progress variable is estimated from the flame brush thickness, δ_B, as:

$$\nabla \widetilde{c} = \frac{\widetilde{c}(1-\widetilde{c})}{\delta_B}. \tag{37}$$

After some calculations, the condition (33) becomes:

$$N_B = \frac{\sigma_y L_y}{g\delta_B} S_T \frac{\tau(1+\tau)}{|\langle \mathbf{u}''.\mathbf{n}\rangle_S|} < 1, \tag{38}$$

evaluated for $\widetilde{c} = 1$. This expression may be simplified by evaluating the turbulent flame speed, S_T, from the integral of the reaction rate over the flame brush. Assuming that $\langle \rho w\rangle_S = \rho_u \langle w\rangle_S$, one obtains:

$$S_T = \frac{g\delta_B}{\sigma_y L_y} \rho_u \langle w\rangle_S. \tag{39}$$

Then the proposed criterion becomes:

$$N_B = \langle w\rangle_S \frac{\tau(1+\tau)}{|\langle \mathbf{u}''.\mathbf{n}\rangle_S|} < 1. \tag{40}$$

A similar analysis, conducted with Eq. (23), leads to a similar criterion:

$$N'_B = \langle w\rangle_S \frac{1+\tau(2+\tau)}{|\langle \mathbf{u}.\mathbf{n}\rangle_S|} < 1. \tag{41}$$

Table 1. Numerical estimates of the proposed criterions from the two available databases

Database	u'	s_L	τ	S_T	$\lvert\langle \mathbf{u}.\mathbf{n}\rangle_S\rvert$ $(\widetilde{c}=1.)$	$\lvert\langle \mathbf{u}''.\mathbf{n}\rangle_S\rvert$ $(\widetilde{c}=1.)$	N_B	N'_B
CTR	3.	1.	3.	1.7	8.	3.	4.	2.
Rutland	1.	1.	2.3	1.8	3.	1.	7.6	3.6

Table 1 provides the values of the numbers N_B and N'_B, for the two available databases, using the assumption $\langle w\rangle_S = s_L$. Both N_B and N'_B are lower in the CTR database (exhibiting GD) than in the Rutland database (with CGD), a result that is consistent with our expectations. Nevertheless, the limiting value is not found to be equal to 1. This is mainly due to some assumptions made in the derivation. In particular, expressions (36) for the flame surface density Σ and (37) for the gradient of the mean progress variable $\widetilde{c}$ are not well verified at the trailing edge of the flame front and only provide an order of magnitude. The criterion is also somewhat approximate because it corresponds only to a necessary condition to have a gradient diffusion transport. Two quantities are not exactly known in this criterion: the surface average of the flame front displacement speed, $\langle w\rangle_S$, which differs in general from the laminar flame speed s_L (see Trouvé & Poinsot 1994); and $\langle \mathbf{u}''.\mathbf{n}\rangle_S$ which probably involves wrinkling scales of the flame front. Nevertheless,

a rough estimate may be made assuming $\langle w \rangle_S = s_L$ and $|\langle \mathbf{u}''.\mathbf{n} \rangle_S| = u'$. Then, the proposed criterion becomes:

$$N_B = \frac{\tau(1+\tau)}{\frac{u'}{s_L}} < 1, \tag{42}$$

which corresponds to a horizontal line in the classical Borghi/Barrère diagram (figure 3). Below this line, corresponding to low turbulence levels, turbulent transport occurs opposite to the direction of mean gradients. Above that line, turbulent transport occurs in the direction of mean gradients. This first simple criterion is also in agreement with the classical analysis of turbulent transport where counter-gradient diffusion is promoted by the increase of the heat release parameter τ (Masuya 1986).

The present analysis should be understood as a first attempt to differentiate between gradient and counter-gradient turbulent diffusion phenomena in premixed flames. The criterion (42) is probably too simple, and the transition between counter-gradient and gradient transport as turbulence levels are increased will not be abrupt and will involve a transition zone. It remains, however, that such a transition will probably occur as supported by our comparison of the two available DNS databases. Future work will be aimed at validating the present analysis and providing a more precise description of the transition between the two situations.

7. Conclusions

We use in this study direct numerical simulations to describe the coupling between the transport equations for mean reaction progress variable, $\widetilde{c}$, and flame surface density, Σ. We are particularly interested in the turbulent transport terms appearing in the equations for $\widetilde{c}$ and Σ since the modeling of those terms remains somewhat controversial: standard gradient transport approximations as proposed in the Coherent Flame Model, or additional transport equations for the turbulent fluxes as proposed in the Bray-Moss-Libby theory. Two different direct numerical simulation databases, the CTR database and the Rutland database, have been used. Both databases correspond to statistically one-dimensional premixed flames in isotopic turbulent flow. The run parameters are significantly different and the two databases correspond to different turbulent combustion regimes (see Fig. 3).

A systematic comparison between the different simulated flames reveals striking differences in their turbulent transport properties. The Rutland case exhibits counter-gradient diffusion of $\widetilde{c}$, a result that is consistent with the Bray-Moss-Libby theory. In contrast, the CTR database features turbulent $\widetilde{c}$-fluxes that are consistent with a gradient transport approximation. In addition, the turbulent diffusion of Σ is found to be strongly correlated to the turbulent diffusion of $\widetilde{c}$. In the Rutland database, counter-gradient diffusion of $\widetilde{c}$ is occurring with counter-gradient diffusion of Σ, whereas in the CTR database, gradient diffusion of $\widetilde{c}$ and Σ is observed. A simple expression proposed by Bray to relate the turbulent flux of Σ to the turbulent flux of $\widetilde{c}$ is found to be valid (Eq. (15)). One important implication of this result is that the modeling of the turbulent flux of $\widetilde{c}$ cannot be made independently of that for the turbulent flux of Σ.

A detailed analysis of all the terms appearing in the conservation equation for the turbulent $\widetilde{c}$-flux, $\widetilde{\overline{\rho}u''c''}$, is also performed. This analysis shows that while pressure effects act to promote counter-gradient diffusion, a result that is consistent with the Bray-Moss-Libby theory, they fail to prevail in the CTR case. Finally, a simple theoretical analysis based on a thin flame model is developed to explain the different turbulent transport properties observed in the CTR and the Rutland simulations. This simple theory distinguishes between situations where the flow field near the flame surface is dominated by the turbulent motions and situations where it is mainly determined by the dilatation occurring within the reaction zone. The CTR simulations belong to the first category, the Rutland simulation to the second. The first category of flames is expected to feature gradient turbulent transport, whereas counter-gradient phenomena will dominate in the second. The analysis also provides a criterion to determine the domain of occurrence of gradient/counter-gradient turbulent transport of $\widetilde{c}$ and Σ (Eq. (42)). This criterion suggests that counter-gradient diffusion is promoted by increasing values of the heat release factor, τ, a result that is consistent with the Bray-Moss-Libby theory as well as by low turbulence levels, whereas gradient diffusion might prevail as turbulence intensities are increased. Future work will be aimed at validating and refining this criterion.

Acknowledgements

The authors wish to thank Prof. C. J. Rutland for providing access to his direct numerical simulation database. The authors acknowledge the fruitful interaction with other members of the combustion group during the summer program. In particular, we thank Prof. C. J. Rutland and Prof. R. S. Cant for many discussions in the course of this study.

REFERENCES

ARMSTRONG, N. W. H. & BRAY, K. N. C. 1992 Premixed turbulent combustion flowfield measurements using PIV and LST and their application to flamelet modeling of engine combustion. *S.A.E. Meeting*, Paper 922322.

BIDAUX, E. & BRAY, K. N. C. 1994 Unpublished work.

BORGHI, R. 1985 On the structure and morphology of turbulent premixed flames. *in Recent Advances in Aerospace Science.* (ed. C. Bruno & C. Casci). Pergamon.

BRAY, K. N. C. 1980 Turbulent flows with premixed reactants. *in Topics in Applied Physics* **44**. Springer-Verlag.

BRAY, K. N. C. 1990 Studies of the turbulent burning velocity. *Proc. R. Soc. Lond. A.* **431,** 315-335.

BRAY, K. N. C., LIBBY, P. A., MASUYA, G. & MOSS, J. B. 1981 Turbulence production in premixed turbulent flames. *Combust. Sci. Tech.* **25,** 127-140.

BRAY, K. N. C., CHAMPION, M. & LIBBY, P. A. 1989 The interaction between turbulence and chemistry in premixed turbulent flames. In *Turbulent Reactive Flows, Lecture Notes in Eng.* **40,** Springer-Verlag.

CANDEL, S. M. & POINSOT, T. 1990 Flame stretch and the balance equation for the flame surface area. *Combust. Sci. Tech.* **70,** 1-15.

CANDEL, S. M., VEYNANTE, D., LACAS, F., MAISTRET, E., DARABIHA, N. & POINSOT, T. 1990 Coherent flame model: applications and recent extensions. *in Series on Advances in Mathematics for Applied Sciences.* World Scientific.

CANT, R. S., POPE, S. B. & BRAY, K. N. C. 1990 Modeling of flamelet surface to volume ratio in turbulent premixed combustion. *Twenty-Third Symp. (International) on Combust. 809-815. The Combustion Institute.*

CHENG, R. K. & SHEPHERD I. G. 1991 The influence of burner geometry on premixed turbulent flame propagation. *Combust. Flame.* **85,** 7-26.

DARABIHA, N., GIOVANGIGLI, V., TROUVÉ, A., CANDEL, S. M. & ESPOSITO, E. 1987 Coherent flame description of turbulent premixed ducted flames. *in Proc. of the France-USA Joint Workshop on Turbulent Combustion.* Springer Verlag.

DUCLOS, J. M., VEYNANTE, D. & POINSOT, T. 1993 A comparison of flamelet models for premixed turbulent combustion. *Combust. Flame.* **95,** 101-117.

FAVRE A., KOVASNAY, L. S. G., DUMAS, R., GAVIGLIO, J. & COANTIC, M. 1976 *La turbulence en mécanique des fluides.* Gauthier Villars.

HAWORTH, D. C. & POINSOT, T. 1992 Numerical simulations of Lewis number effects in turbulent premixed flames. *J. Fluid Mech.* **244,** 405-436.

LAUNDER, B. E. 1976 Heat and mass transport by turbulence. *in Topics in Applied Physics* **12**. Springer-Verlag.

LIBBY, P. A. & BRAY, K. N. C. 1981 Countergradient diffusion in premixed turbulent flames. *AIAA J.* **19,** 205-213.

MAISTRET, E., DARABIHA, N., POINSOT, T., VEYNANTE, D., LACAS, F., CANDEL, S. M. & ESPOSITO, E. 1989 Recent developments in the coherent flamelet description of turbulent combustion. In *Proc. 3rd Int. SIAM Conf. on Numerical Combustion.*

MARBLE, F. E. & BROADWELL, J. E. 1977 The coherent flame model for turbulent chemical reactions. *Project Squid Technical Report.* TRW-9-PU.

MASUYA G. 1986 Influence of Laminar Flame Speed on Turbulent Premixed Combustion. *Combustion and Flame.* **64,** 353-367

MOSS J. B. 1980 Simultaneous Measurements of Concentration and Velocity in an Open Premixed Turbulent Flame. *Combust. Sci. Tech.* **22,** 119-129.

PETERS, N. 1986 Laminar flamelet concepts in turbulent combustion. *Twenty-First Symp. (International) on Combust.* 1231-1250. The Combustion Institute.

PETERS, N. 1992 A spectral closure for premixed turbulent combustion in the flamelet regime. *J. Fluid Mech.* (Submitted for publication).

POINSOT, T., VEYNANTE, D. & CANDEL, S. M. 1991 Quenching processes and premixed turbulent combustion diagrams. *J. Fluid Mech.* **228,** 561-605.

POPE, S. B. 1988 Evolution of surfaces in turbulence. *International J. Engng. Sci.* **26,** 445-469.

RUTLAND, C. J. & TROUVÉ, A. 1993 Direct simulations of premixed turbulent flames with non-unity Lewis numbers. *Combust. Flame.* **94,** 41-57.

RUTLAND, C. J. & CANT, R. S. 1994 Turbulent transport in premixed flames. *Proc. of the Summer Program*, Center for Turbulence Research, NASA Ames/ Stanford Univ.

SHEPHERD, I. G., MOSS, J. B. & BRAY, K. N. C. 1982 Turbulent transport in a confined premixed flame. *Nineteenth Symp. (International) on Combust.* 423-431. The Combustion Institute.

TROUVÉ, A. & POINSOT, T. 1994 The evolution equation for the flame surface density in turbulent premixed combustion. *J. Fluid Mech.* **278,** 1-31.

WILLIAMS, F. A. 1985 *Combustion theory.* 2nd ed., Benjamin Cummings.